ASTRONOMY & ASTROPHYSICS
SUPPLEMENT SERIES

Astron. Astrophys. Suppl. Ser. **126,** 21-30 (1997)

Radial velocities, rotations, and duplicity of a sample of early F-type dwarfs⋆

B. Nordström[1,2], R.P. Stefanik[2], D.W. Latham[2], and J. Andersen[1,2]

[1] Astronomical Observatory, Niels Bohr Institute for Astronomy, Physics & Geophysics, Juliane Maries Vej 30, DK - 2100 Copenhagen, Denmark
[2] Harvard-Smithsonian Center for Astrophysics, 60 Garden Street, Cambridge, MA 02138, U.S.A.

Received October 9, 1996; accepted February 17, 1997

Abstract. We present new radial and rotational velocities for 595 nearby early F dwarfs, based on digital spectra cross-correlated with individually optimised synthetic template spectra. The selection of optimum templates, the determination of rotational velocities, and the extraction of velocities from the blended spectra of double-lined spectroscopic binaries are discussed in some detail. We find 170 spectroscopic binaries in the sample and determine orbits for 18 double-lined and 2 single-lined binaries, including some spectroscopic triples. 73 stars are listed with too rapid rotation to yield useful radial velocities (i.e. $v \sin i > 120$ km s^{-1}). We discuss the binary frequency in the sample, and the influence of unrecognised binaries on the definition of clean metallicity groups of young F dwarfs and the determination of their kinematical properties.

Key words: methods: statistical — techniques: radial velocities — stars: binaries: spectroscopic — stars: kinematics — Galaxy: solar neighbourhood

1. Introduction

Positions, velocities, metallicities, and ages of stars are the raw material from which samples of the stellar populations in the Milky Way galaxy are defined. Correlations between these parameters provide clues to the chemical and dynamical evolution of our home galaxy. Yet, after decades of observation and study, controversy remains concerning the true relationships between these basic observational parameters even for the solar neighbourhood, and even more so concerning their interpretation. Thus, as models of the formation and evolution of the galactic disk improve, the need for more definitive observational data becomes ever more pressing.

Coordinated efforts are being made towards this goal on two fronts: On the one hand, the chemical evolution of nearby solar-type stars has been studied in detail by Edvardsson et al. (1993; E93) using high-resolution spectroscopy. In parallel, a major programme has been undertaken to complete an inventory of the solar neighbourhood in order to define large, homogeneous, complete, and kinematically unbiased samples of nearby F and G dwarf stars (see, e.g. Strömgren 1987; Nordström et al. 1996). Sample selection is based on the all-sky $uvby-\mathrm{H}\beta$ photometry by Olsen (1983, 1993, 1994a,b), which allows the determination of distances, metallicities and individual ages. PPM proper motions (Bastian & Röser 1991-1993) have been improved using modern positions observed with the Carlsberg Automatic Meridian Circle (Carlsberg 1991-1994). Finally, multiple radial-velocity observations have been obtained of the F and G dwarfs in the sample, mostly with the CORAVEL scanners (Mayor 1985). Altogether, complete data have now been collected for some 10 000 stars in both hemispheres. The programme is further described in Nordström et al. (1996).

Different subgroups of these stars are interesting for a variety of purposes. At the old, metal-poor end of the sample, the delineation and characterisation of the old thin disk, thick disk, and halo populations are the main interest. On the other hand, the early F dwarfs for which reliable ages and metallicities can be determined, but which are too young to have moved far from their place of formation, are of prime importance in clarifying the cause(s) of the scatter in the local age-metallicity diagram (see Sect. 5). In all cases, radial velocities are needed in order to compute space motions and galactic orbits for individual stars. In addition, repeated radial-velocity observations allow the detection of spectroscopic binaries. This is

Send offprint requests to: B. Nordström (Danish address): E-mail: birgitta@astro.ku.dk

⋆ Tables 1, 5 and 6 are only available, and Tables 2-4 also available in electronic form at the CDS via anonymous ftp to cdsarc.u-strasbg.fr (130.79.128.5) or via http://cdsweb.u-strasbg.fr/Abstract.html

important because large-amplitude binaries might bias the kinematical parameters derived for the samples of stars to which they belong. In addition, unrecognised binaries with significant amounts of secondary light of a colour different from that of the primary may be classified incorrectly when photometric age or metallicity indicators are used to subdivide the initial sample. Detecting such binary systems and analysing their composite spectra is the first step in correcting for these effects.

The class of early F-type dwarfs contains a large proportion of rapidly rotating stars ($v \sin i > 40$ km s^{-1}), for which radial velocities cannot be accurately determined with CORAVEL. We have therefore observed that part of our local sample with the Center for Astrophysics (CfA) Digital Speedometers (Latham 1985, 1992), which can handle rotations up to ∼120 km s^{-1}(Nordström et al. 1994; Paper I), in order to determine their radial and rotational velocities and search for binaries in the sample.

The present paper describes the selection of the sample and our observation and reduction procedures, gives results for 595 stars, including preliminary spectroscopic orbits for 18 double-lined and 2 single-lined binaries, and discusses the binary frequency in the sample and the extent to which such binaries may have been inadvertently included in the sample. Several forthcoming papers will further discuss the evolution of the galactic disk, based on the full data set (see, e.g. Nordström et al. 1997).

2. Sample selection

From the catalogue by Olsen (1983) of four-colour photometry of all A5-G0 stars in the HD catalogue to $m_v = 8.3$, those F stars were selected which have evolved sufficiently off the ZAMS (i.e. by roughly $0.5-2.0$ mag in M_v) that individual ages can be determined from comparisons with theoretical isochrones. The following overall criteria were used (the precise δc_1 limit varying from 0.18 to 0.12 with $b-y$ within this range):

$0.219 < b-y < 0.391$

$0.066 < \delta c_1 < 0.15$.

Except that the selection of stars took place before Hβ photometry was complete for all the stars, these criteria are quite similar to those used by E93 to define their sample of stars.

As the CORAVEL observations got under way it was realized, however, that over half of the stars with $b-y < 0.27$ were rotating too rapidly to yield usable radial velocities. The stars in the colour range $0.219 < b-y < 0.270$ and north of declination $-40°$ were therefore transferred to the CfA instruments, together with a few later-type stars that were also rotating too rapidly for CORAVEL (and are found here to be short-period binaries). There is, however, enough overlap with the early CORAVEL results to ensure good consistency of the radial-velocity zero-points of the two systems.

Of the 669 stars on the original observing list (26% of all stars in the Olsen catalogues in the same colour range and over the whole sky), results are presented here for a total of 595 stars (Tables 1 and 2), while 73 proved to be rotating too rapidly even for the CfA technique ($v \sin i > 120$ km s^{-1}); for completeness, these stars are listed in Table 4. A new, precise spectroscopic orbit for the double-lined eclipsing binary EI Cep, which is included in the photometrically defined sample, will be published separately.

3. Observations and data reduction

Echelle spectra for all programme stars were obtained with the 1.5-m Wyeth reflector at the Oak Ridge Observatory in Harvard, Massachusetts, the 1.5-m Tillinghast reflector on Mt. Hopkins, Arizona, and occasionally with the Multiple Mirror Telescope, also at Mt. Hopkins. Echelle spectra covering the range $5165.77 - 5211.25$ Å were obtained with the nearly identical CfA echelle spectrograph systems at all three telescopes and recorded with photon-counting intensified Reticon detectors. The instruments and standard observing and reduction procedures are described by Latham (1985, 1992). Standard observing procedures were followed throughout, but with increased exposure levels for the more rapidly-rotating stars which need better signal-to-noise in order to ensure reliable velocities.

For the determination of radial velocities from these spectra for stars with a wide range of rotations, we have developed a digital cross-correlation procedure based on the XCSAO task (Kurtz et al. 1992) as implemented in the IRAF environment[1], using a large grid of synthetic template spectra covering the ranges in effective temperature, gravity, and rotation of our programme stars. The details of our technique and its performance have been documented in Paper I and will not be repeated here. We comment briefly below on its practical application to the programme stars, and on two refinements in the technique implemented since Paper I.

The grid of synthetic template spectra used here was computed for [Fe/H] = 0.0, as the m_1 index for the programme stars indicated that they all have metallicities sufficiently close to solar. Effective temperatures range from 6000 to 7000 K in steps of 250 K, $\log g$ from 4.5 to 3.0 in steps of 0.5 dex, and $v \sin i$ from 0 to 100 km s^{-1} in steps of 10 km s^{-1} and from 100 to 200 km s^{-1} in steps of 20 km s^{-1}. Optimum templates were selected for the individual programme stars as follows:

For the stars with known Hβ indices and reddenings (about 3/4 of the sample), Dr. E.H. Olsen kindly computed the individual $T_{\rm eff}$ and $\log g$ values, using the Magain (1987) calibration for $T_{\rm eff}$ and a procedure similar

[1] IRAF is distributed by the National Optical Astronomy Observatories, which are operated by the Association of Universities for Research in Astronomy under cooperative agreement with the National Science Foundation.

Table 2. Data for stars with double-lined or composite spectra. Coordinates are for equinox J2000; V_0 and m.e. in km s^{-1}, and Span in days

HD	RA	Dec	Temp1	Temp2	α	n	V_0	m.e.	Span	q	m.e.	Rem.
5153	00:53:36.9	+24:55:58	7250/010	7000/010	0.65	3	−24.61	0.29	780	0.926	0.015	SB2W
5843	01:00:13.1	+11:56:07	7000/010	6750/010	0.73	25	−5.64	0.24	1471	0.921	0.018	SB2O
6469	01:06:08.4	+35:30:58	7250/120	6750/000	0.06	6	12.76	2.66	1290			SB2C
8026	01:20:47.7	+56:12:28	7250/120	6750/000	0.07	5	−0.28	1.01	1809			SB2C
8136	01:22:39.8	+68:33:55	6750/010	6750/010	0.87	8	−19.48	1.29	1128	1.101	0.045	SB2W
10629	01:44:30.7	+39:57:30	7000/120	7000/030	0.41	3	−4.08	1.20	1028			SB2C
12180B	01:58:60.0	−22:55:03	6500/000	6500/000	1.00	3	29.46	0.23	751	0.976	0.014	SB2W
12637	02:04:45.8	+39:26:06	7250/100	6750/000	0.11	11	6.13	1.00	1298			SB2C
12984	02:07:01.8	−04:13:03	6750/080	6750/010	0.15	3	−14.56	6.89	753	0.952	0.665	SB2W
14124	02:19:21.6	+60:29:10	7250/120	6750/000	0.39	5	−1.16	0.72	1701			SB2C
15227	02:27:32.0	+16:38:36	6750/000	6750/000	0.93	8	13.39	0.20	1446	0.978	0.019	SB2W
17613B	02:49:52.2	+08:56:16	6000/000	5750/000	0.37	6	2.26	0.40	820	0.875	0.062	SB2W
19115	03:03:59.9	−17:44:16	6750/030	6500/030	0.49	3	37.16	2.94	764	0.877	0.122	SB2W
22054	03:32:13.1	−31:34:13	6750/000	6500/000	0.66	10	17.44	0.89	1090	0.914	0.037	SB2O
24623	03:54:34.9	−09:31:13	6750/000	6500/000	0.66	22	9.47	0.09	1452	0.982	0.004	SB2O
36845	05:33:43.5	−18:40:42	6750/100	6500/000	0.14	7	38.23	1.33	1741			SB2C
37038	05:35:32.4	−01:50:46	7000/100	6750/000	0.23	9	17.06	0.38	1777			SB2C
37603A	05:40:18.1	+15:21:01	7000/000	6750/000	0.80	10	21.01	0.73	1087	1.029	0.040	SB2W
37603B	05:40:18.1	+15:21:01	7000/000	6750/000	0.58	18	20.62	0.38	1087	0.938	0.052	SB2O
39166	05:54:03.5	+57:02:44	7000/000	7000/000	0.91	25	9.01	0.12	1800	0.997	0.006	SB2O
44849	06:28:21.9	+62:42:44	7250/100	6750/010	0.13	4	16.68	1.07	1044			SB2C
54901	07:11:16.8	+15:19:56	7000/020	6500/000	0.17	24	−9.86	0.15	1796	0.761	0.011	SB2O
57769	07:24:17.2	+36:18:38	6750/090	6750/010	0.09	11	−34.31	3.08	1800			SB2C
63424	07:47:10.1	−39:06:12	6750/000	6750/000	0.73	3	−0.50	0.18	736			SB2C
74425	08:47:50.8	+66:12:38	6000/050	6000/040	0.50	16	16.88	0.35	1321	0.857	0.009	SB2O
75638	08:51:26.3	+12:07:32	7000/080	6750/010	0.10	13	11.05	0.91	1346			SB3O
76702	09:07:58.0	+81:02:28	7000/100	6500/010	0.04	6	6.38	1.32	1188			SB2C
80853	09:21:10.3	−35:21:25	7000/100	6750/010	0.07	7	24.50	0.67	1211			SB2C
85294	09:50:41.0	−07:22:56	7000/090	6750/010	0.07	9	28.36	1.70	1500	0.661	0.064	SB2W
86579	09:59:18.5	−03:04:29	7000/100	6750/010	0.11	7	7.26	1.42	1788	1.404	0.951	SB2W
87810	10:07:07.6	−21:15:20	6750/000	6750/000	1.00	23	−0.24	0.07	1536	0.997	0.004	SB2O
88162	10:10:22.6	+20:56:43	6750/010	6750/010	0.83	20	−27.67	0.15	1774	0.952	0.022	SB2O
88788	10:14:19.5	−12:35:03	7000/120	6500/010	0.07	6	2.75	1.95	1479			SB2C
92197	10:38:59.4	+15:58:59	6750/010	6750/010	0.80	6	8.88	2.11	1791	0.671	0.187	SB2W
93785	10:49:15.0	−26:48:55	7000/120	6750/030	0.33	5	21.18	2.59	1502			SB2C
94034	10:50:44.3	−34:29:11	6750/010	6750/010	0.91	5	6.03	0.26	797	1.098	0.051	SB2W
96050	11:04:31.9	−21:07:35	6750/010	6750/010	0.87	4	6.31	1.28	1433	0.962	0.043	SB2W
104636	12:02:59.9	+41:03:55	7000/100	7000/000	0.09	12	3.56	1.41	1216			SB2C
108100	12:24:56.9	+42:51:17	7000/080	6750/020	0.17	7	−7.76	1.04	1796			SB2C
109557	12:35:42.7	−16:49:34	7000/100	6750/020	0.24	5	1.09	1.26	1765			SB2C
110606	12:43:40.4	−35:24:50	7000/020	7000/010	0.81	5	4.74	0.28	790	0.912	0.034	SB2W
121648	13:56:09.5	+25:55:07	6750/010	6750/010	0.86	30	−29.50	0.27	1947	0.976	0.010	SB2O
128901	14:37:46.2	+52:01:57	7000/010	7000/010	0.75	7	7.69	7.42	1624			SB2C
131773	14:56:21.6	−29:57:36	7000/080	6750/000	0.12	4	−9.88	0.69	830			SB2C
134193	15:08:56.7	−11:47:25	6750/010	6750/010	0.56	13	4.77	0.22	1208	0.884	0.009	SB2O
135100	15:11:26.6	+48:41:34	6750/020	6750/010	0.67	6	−14.84	0.18	1656	0.944	0.008	SB2W
136276	15:20:09.3	−13:11:30	6750/010	6750/010	0.45	5	−12.67	0.67	1209	0.828	0.024	SB2W
147428	16:20:16.9	+40:15:33	6750/030	6500/010	0.18	19	−19.66	0.18	1620	0.709	0.018	SB2O
155025	17:07:59.1	+27:06:05	7000/020	7000/000	0.46	8	−16.78	1.55	1291	1.027	0.163	SB2W
156458	17:17:36.9	+01:44:32	6750/010	6750/010	0.39	15	−30.65	0.18	1584	0.961	0.053	SB2O
159172	17:33:58.9	−17:50:10	6500/010	6500/000	0.38	15	2.60	0.58	1484	0.822	0.027	SB2O
171275	18:32:17.1	+36:25:34	7000/030	7000/020	0.29	28	−30.87	0.18	1540	0.824	0.010	SB2O
176409	18:56:55.1	+56:44:58	7000/100	6750/000	0.04	8	−28.30	1.57	1573			SB2C
176613	19:02:19.6	−29:20:30	7000/010	7000/010	0.90	4	−1.76	0.32	1327	0.968	0.023	SB2W

to that of Edvardsson et al. (1993) for log g. The set of templates closest to these values was selected for each of these stars. For the remainder, we assumed $T_{\rm eff} = 7000$ K and log $g = 4.0$ as our previous tests have shown these to be adequate (Paper I).

The optimum template rotation cannot be defined from the photometry, but must be found from test correlations of the observed spectra with the appropriate set of rotating templates. In Paper I, optimum template selection was based on the goodness-of-fit parameter R (cf. Kurtz et al. 1992). As noted there, however, this criterion fails in the numerous cases of composite spectra. Considerable further experimentation led us to the conclusion that the maximum height of the correlation peak

Table 2. continued

HD	RA	Dec	Temp1	Temp2	α	n	V_0	m.e.	Span	q	m.e.	Rem.
177005	19:01:14.7	+35:37:25	7000/010	7000/010	0.19	13	2.79	0.49	1560	0.739	0.024	SB2O
192327	20:14:19.9	+00:08:39		7000/000		8	−32.85	0.49	1409			SB2C
194032	20:22:20.4	+29:05:26		7000/000		11	−29.95	0.55	1596			SB2C
195147	20:10:55.5	+84:32:40	7000/020	7000/010	0.50	4	−11.81	0.89	1061	0.868	0.044	SB2W
198226	20:48:06.2	+27:27:24	6750/030	6750/040	0.70	21	−16.03	2.25	1471			SB3O
203031	21:19:00.1	+26:05:23	7000/050	7000/010	0.22	21	6.43	0.19	1474	0.677	0.015	SB2O
205798	21:36:53.8	+33:43:06	7000/050	7000/040	0.25	10	−25.47	1.10	1419	0.277	0.014	SB2W
211244	22:15:26.6	+18:36:11	7000/070	7000/060	0.75	7	2.43	1.11	1386	0.895	0.025	SB2W
215306	22:43:48.8	+27:41:01	7000/100	7000/010	0.25	7	−11.66	0.55	1505			SB2C
221431	23:32:18.4	−33:40:32	7000/020	7000/000	0.34	6	−4.35	0.10	1377	0.898	0.005	SB2W
222995	23:45:37.1	+13:09:09	6750/040	6750/000	0.30	19	−20.28	0.25	1507	0.770	0.025	SB2O

Table 3. Orbital elements for spectroscopic binaries with orbital solutions. Mean errors are indicated below each parameter

HD	P [d]	T [HJD-2 440 000]	V_0 [km s^{-1}]	K_1 [km s^{-1}]	K_2 [km s^{-1}]	e	ω [°]	σ_1, σ_2 [km s^{-1}]
005843	9.17607	7868.883	−5.64	73.00	79.26	0.005	185.2	1.18
	0.00016	1.792	0.24	0.33	1.35	0.004	70.4	4.96
022054	10.41302	7478.887	17.44	71.17	77.90	0.129	130.6	5.89
	0.00038	0.146	0.89	2.40	0.78	0.010	4.3	0.91
024623	19.66227	7861.470	9.47	63.92	65.08	0.491	130.0	0.53
	0.00037	0.014	0.09	0.19	0.22	0.002	0.3	0.64
037603B	27.76205	7886.104	20.62	20.43	21.79	0.405	349.6	2.71
	0.00621	0.226	0.38	0.88	0.66	0.024	4.1	1.95
039166	15.86860	7568.472	9.01	61.97	62.16	0.232	304.3	0.75
	0.00037	0.034	0.12	0.26	0.27	0.003	0.8	0.80
054901	41.00333	7709.088	−9.86	44.46	58.45	0.638	349.3	0.72
	0.00125	0.024	0.15	0.26	0.72	0.004	0.5	2.36
074425	1.585232	7797.961	16.88	101.93	118.97	0.011	184.0	1.77
	0.000008	0.100	0.35	0.64	0.79	0.005	22.6	2.19
075638	5.81667	7558.279	11.05	28.92		0.083	322.0	2.96
	0.00086	0.452	0.91	1.20		0.056	28.2	
087810	12.94724	7442.274	−0.24	55.50	55.68	0.439	48.6	0.47
	0.00012	0.008	0.07	0.17	0.18	0.002	0.3	0.49
088162	24.74771	7764.323	−27.67	23.85	25.05	0.603	17.4	0.78
	0.00310	0.038	0.15	0.32	0.44	0.009	0.93	1.10
121648	4.99167	7750.057	−29.50	89.85	92.02	0.007	219.4	1.86
	0.00003	0.512	0.27	0.56	0.72	0.004	36.9	2.39
134193	5.76930	7572.411	4.77	77.40	87.61	0.004	73.7	1.14
	0.00006	0.930	0.22	0.50	0.48	0.005	57.9	1.07
147428	75.55870	7784.165	−19.66	27.28	38.46	0.089	186.7	0.70
	0.02198	1.059	0.18	0.25	0.83	0.014	5.3	2.71
156458	17.11603	7990.970	−30.65	60.58	63.07	0.161	279.1	0.54
	0.00030	0.078	0.18	0.24	3.06	0.004	1.7	8.74
159172	13.87687	7674.910	2.60	54.89	66.78	0.218	204.1	3.61
	0.00033	0.055	0.58	1.49	0.37	0.010	1.8	0.75
171275	15.40365	7839.525	−30.87	58.78	71.37	0.083	305.4	0.91
	0.00058	0.116	0.18	0.23	0.73	0.005	2.9	2.91
177005	11.10549	7943.389	2.79	53.24	72.04	0.333	143.3	2.86
	0.00063	0.078	0.49	1.52	1.53	0.011	2.6	1.93
198226	1.49941	7773.106	−16.03	90.51		0.021	93.7	10.1
	0.00004	0.421	2.25	3.27		0.034	101.3	
203031	48.73828	7760.086	6.43	27.49	40.59	0.493	159.0	1.29
	0.00442	0.080	0.19	0.53	0.55	0.009	1.0	1.11
222995	85.83454	7819.892	−20.28	31.73	41.20	0.335	175.0	2.17
	0.02771	0.392	0.25	0.86	0.51	0.008	1.8	1.18

is a more reliable criterion for choosing the rotating template which gives the best match to the observed spectra, and this method was adopted for the final correlations of all programme stars.

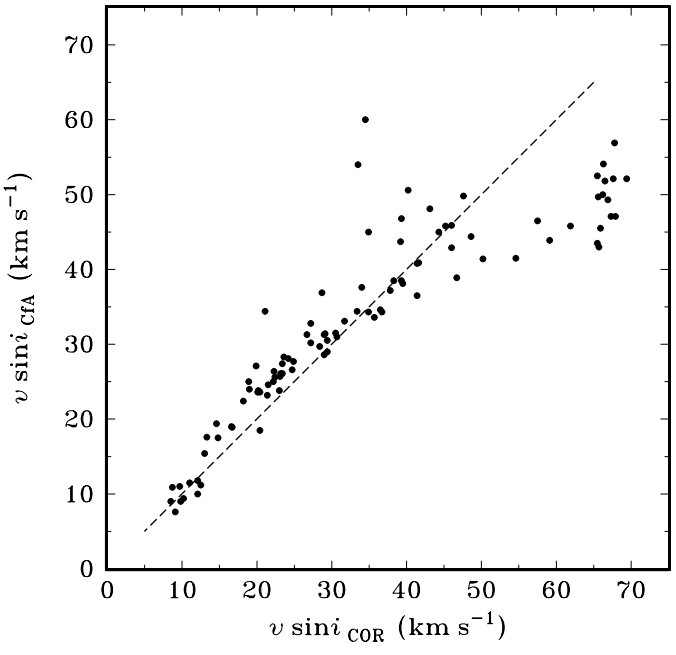

Fig. 1. Rotational velocities (km s^{-1}) derived here vs. those observed with CORAVEL

From the correlation peak height as a function of template rotation, the value corresponding to maximum correlation height was estimated by quadratic interpolation. As shown in Fig. 1, this procedure leads to much better agreement with the CORAVEL rotations measured for the overlap of slowly-rotating stars common to the two programmes which was discussed in Paper I. The overall zero-point and scale differences in $v \sin i$ seen with the older procedure have disappeared, although there still seems to be a difference of $\sim$3 km s^{-1} for rotations around 20 km s^{-1}. Given the uncertainties in the treatment of the instrumental profile and scattered light of our data and the simplifying assumptions underlying the calibration of both methods, the origin of this difference is not clear, but it remains within the fundamental uncertainty of $\sim$10% derived by Collins & Truax (1995). The increased scatter seen for $v \sin i > 40$ km s^{-1} is presumably due to the rapidly deteriorating accuracy of the CORAVEL rotations for such broad-lined stars, due to the fixed CORAVEL mask which is optimised for sharp-lined stars.

We have verified that our radial-velocity zero-point, which was the key subject of Paper I, remains the same to within 100 m s^{-1} when using this modified procedure. Thus, our previous results on the systematic and random errors of our radial velocities remain valid for the data presented here.

The second refinement in our technique was the use of the two-dimensional cross-correlation algorithm TODCOR (Zucker & Mazeh 1994), as implemented at CfA by G. Torres, to extract radial velocities of both components from the observed, blended spectra of 65 double-lined spectroscopic binaries in our sample. For 18 of these systems we had enough velocities to allow solutions for double-lined orbits, and in another 21 cases the available pairs of primary and secondary velocities spanned a sufficient velocity range that we could use the Wilson (1941) method to derive systemic velocities and mass ratios.

The ability of TODCOR to extract reliable velocities even from strongly blended correlation peaks is quite remarkable, if a suitably fine grid of rotating templates is available. The absence of systematic velocity errors has been checked in a system with equal components by Latham et al. (1996). As an application of particular value in the present programme, we have been able to derive velocities with TODCOR for a considerable number of systems composed of rapidly-rotating late A-type primaries and sharp-lined late-type secondaries contributing only a few percent of the total light. For these systems the standard correlations against slowly-rotating templates only picked up the velocity of the slowly-rotating secondary. With TODCOR we were able to identify the spectrum of the rapidly-rotating primary and to solve for the velocities of both stars.

TODCOR can also provide an estimate of the light ratio L_2/L_1 between the two stars at the wavelength observed. We list this information when available, but have not performed a similarly exhaustive study of its accuracy as for the radial velocities, including, e.g., template optimization for the individual binary components.

4. Results

Table 1 (available in electronic form only; see footnote to title page) gives our main results for the 530 single-lined stars for which reliable radial velocities could be obtained (all velocity data in km s^{-1}).

In Table 1, Cols. 1-3 give HD numbers and J2000 coordinates, Col. 4 indicates the atmospheric parameters of the adopted synthetic template spectrum (t followed by the temperature and g by 10 $\times$ log g), and Col. 5 the rotational velocity of the star determined as described above.

Columns 6 and 7 give the number of observations, n, and the time span (days) between the first and last observation.

Columns 8-13 list, respectively, the mean radial velocity and its standard error, the standard deviation of the individual velocities, the average uncertainty of a single observation as computed by XCSAO (see Paper I), the ratio of observed to expected rms error, the observed χ^2 and the probability $P(\chi^2)$ that it is due to the random errors of n observations of an otherwise constant star. If the observed standard deviation is less than predicted by

XCSAO (which often happens by chance when small numbers of observations are involved), the error of the mean velocity is given as the latter divided by $\sqrt{n}$. Columns 14 and 15 list, for reference, the average values of the goodness-of-fit statistic $< R >$ (Kurtz et al. 1992) and the height of the correlation peak.

Results for the 65 double-lined systems treated with TODCOR are given in Table 2. The first three columns are as in Table 1, while Cols. 4 and 5 give the parameters of the two templates (i.e. temperature and rotation; $\log g = 4.0$ in all cases). Column 6 lists the mean luminosity parameter $\alpha = L_2/L_1$ provided by TODCOR, and Col. 7 the number of observations. The systemic velocity and its mean error are given in Cols. 8-9, derived, in order of preference, from a full orbital solution, from the available pairs of primary and secondary velocities using the Wilson (1941) method (in which the systemic velocity and mass ratio are derived from a fit of V_2 vs. V_1, assuming only momentum conservation), or as a straight mean. For systems with an orbital solution or analysed by the Wilson method, the mass ratio (q) and its mean error are given in the following two columns. The remarks in the final column indicate double-lined (SB2) or triple (SB3) systems with either no significant velocity variation observed (C), analysed by the Wilson method (W), or with an orbital solution (O). For the triple systems, only a single-lined orbit for the short-period pair has been determined.

Table 4. Stars which rotate too rapidly for usable radial-velocity measurements with the CfA instruments

HD	HD	HD	HD	HD
4086	27832	81725	125488	181656
4856	30315	84667	127457	182246
6696	36844	88829	130353	190004
7138	38610	89866	130667	196386
8302	38753	91728	131160	198028
8607	42313BC	94206	131721	198047
11284	46318	99946	135282	198346
13179	51832	103846	141652	203405
16453	54269	104622	142124	212048
17613A	63795	110220	145873	213619
18570	72984	110456	150340A	217855
19759	74781	111005	166600	218010
23290	77214	118703	168066	219712
26757	79725	119603	179280	
27743	80678	121136	180005	

The elements of the 18 double-lined and 2 single-lined spectroscopic orbits derived here are given in Table 3, and the orbits are shown in Fig. 2. The 73 stars rotating more rapidly than 120 km s^{-1} and for which no velocities could be obtained are listed in Table 4 (HD numbers only).

Finally, the individual radial-velocity observations for single-lined and double-lined stars are listed in Tables 5 and 6, respectively (provided in electronic form only).

5. Discussion

The immediate result of this paper is the catalogue of 595 mean radial velocities and derived quantities contained in Tables 1 and 2. As shown in Fig. 3, the typical mean error of the mean velocity of a constant star is $\sim$1 km s^{-1} for stars rotating less than $\sim$120 km s^{-1}.

As our criterion for identifying spectroscopic binaries in the sample we adopt the limit $P(\chi^2) \leqq 0.01$ for significant radial-velocity variability, i.e. a confidence level of 99%. The distribution of observed $P(\chi^2)$ values is displayed in Fig. 4 and shows a prominent peak of 170 stars in the bin $0.00 - 0.01$ in $P(\chi^2)$, corresponding to the spectroscopic binaries. It is also noteworthy, however, that the $P(\chi^2)$ distribution remains essentially flat in the entire range $0.01 - 1.00$, indicating that the internal error estimates from XCSAO which were used to compute χ^2 are indeed realistic. If one relaxes the variability criterion to $P(\chi^2) \leqq 0.04$, the number of stars satisfying this criterion increases to 199.

The bins $0.00 - 0.04$ in Fig. 4 still contain a random component of constant stars, corresponding to the average level in the rest of the $P(\chi^2)$ range, 4.1 stars per bin of 0.01 in $P(\chi^2)$. Hence, the 170 stars in the first bin should be reduced to 166, and the 29 stars in the next three bins to 17, giving a range for the true number of detected binaries of $166 - 182$, with a sampling error of $\sim$13. The observed binary frequency is thus $29 \pm 2\%$.

The raw binary fraction derived above must be corrected for the fact that our sample is limited by apparent magnitude, thus favouring the inclusion of binaries which are, on average, more luminous than the single stars. Suppose, as an example, that our double-lined binaries (Table 2) were on average 50% more luminous than single stars of the same colour. We would then include them from a volume that is a factor 1.84 larger than that in which the single stars are complete. Under this assumption, 30 of these stars would be removed from the sample for this reason, reducing the true frequency of detected binaries to $24 \pm 2\%$. A similar effect will operate on the $\sim$100 single-lined systems since the light of the secondaries will be present at some level, but we estimate that $\sim$10% is a plausible rough upper limit to their contribution. This suggests that fewer than $\sim$15 single-lined binaries have been included from outside our completeness limit for single stars, reducing our estimate of the true frequency of detected binaries to perhaps $22 \pm 2\%$.

A similar analysis of the $P(\chi^2)$ distribution of the Duquennoy & Mayor (1991) volume-limited sample of G dwarfs (their Fig. 3) yields a fraction of radial-velocity variables of $\sim$37%. If the true frequency of spectroscopic binaries is the same in the two samples, these figures

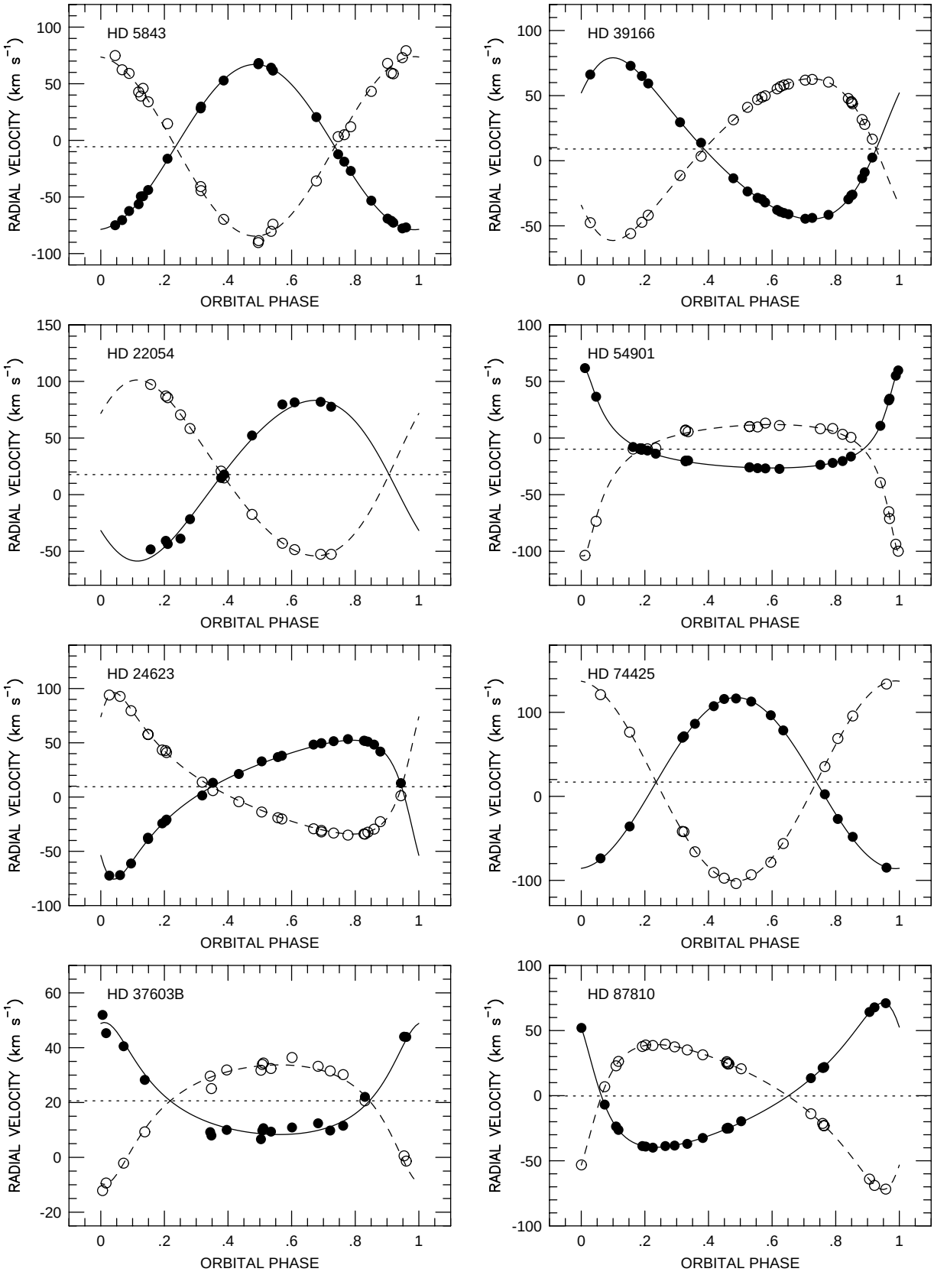

Fig. 2. Spectroscopic orbits and observed radial velocities for 20 binary systems. The orbital elements are given in Table 3

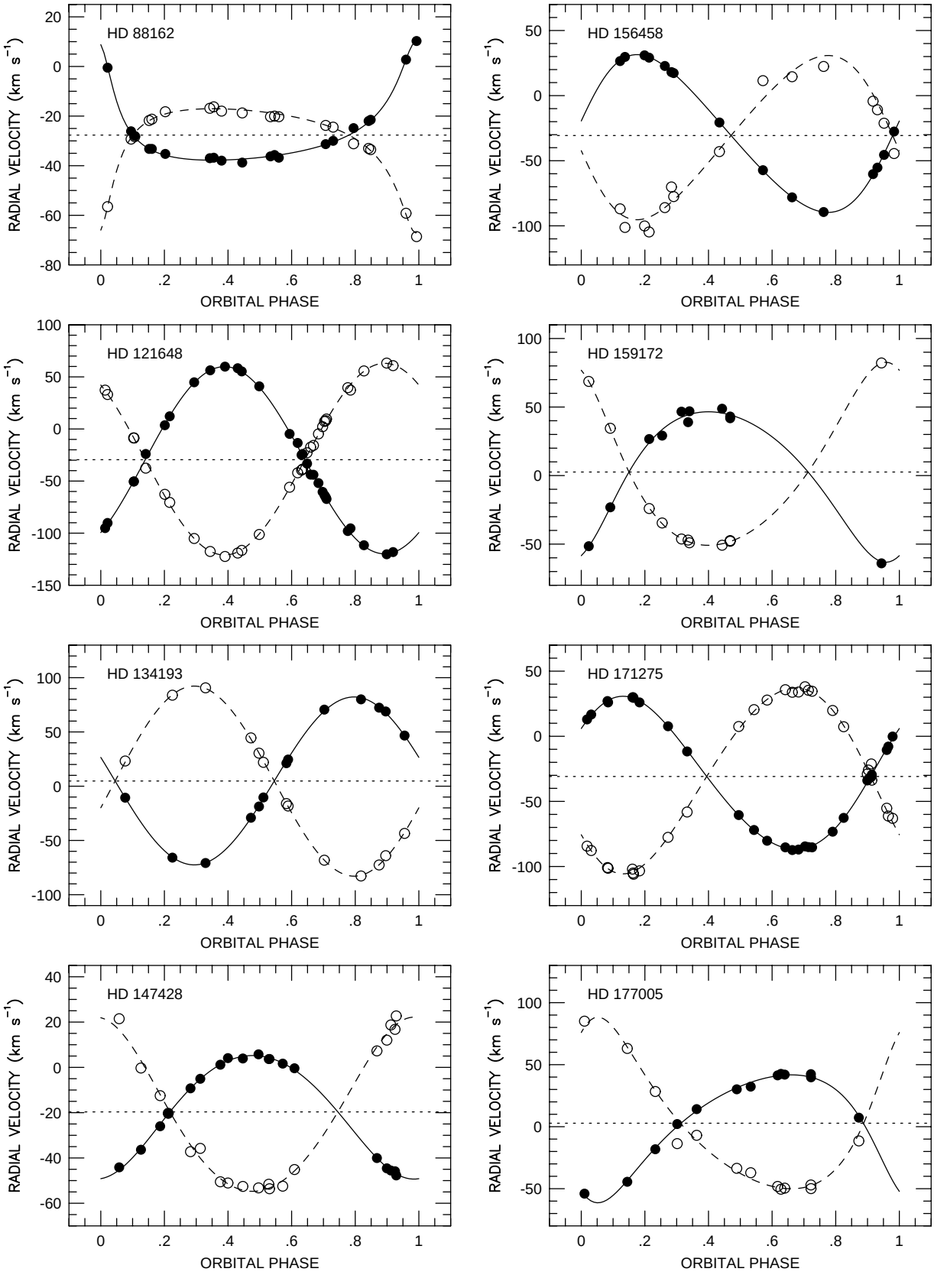

Fig. 2. continued

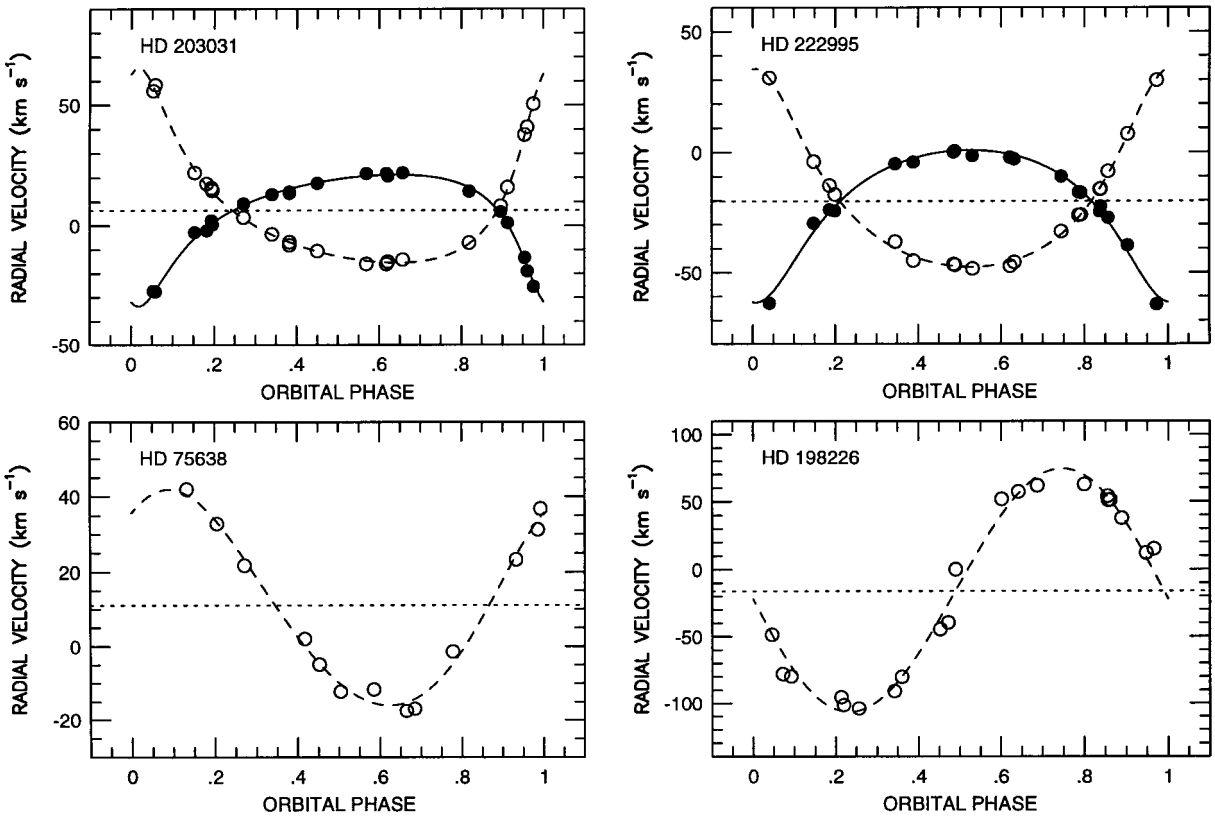

Fig. 2. continued

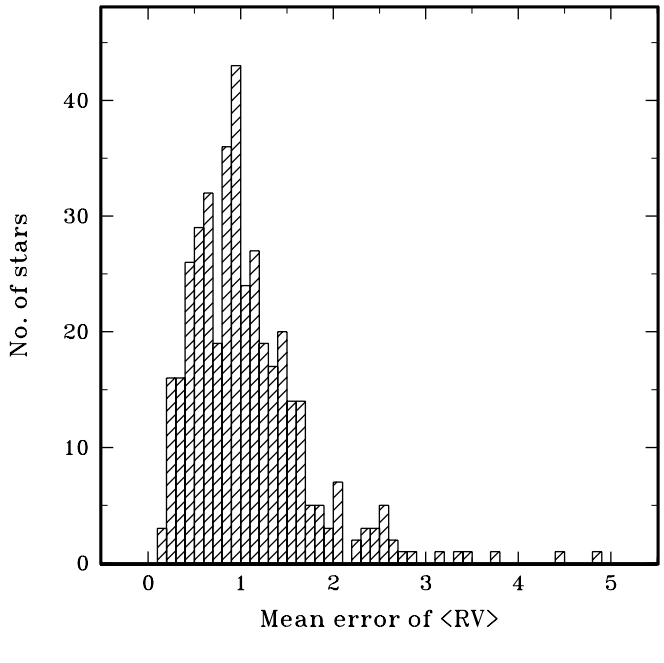

Fig. 3. Distribution of mean errors (km s^{-1}) of the mean velocities of the 426 constant stars from Table 1 (defined by the criterion $P(\chi^2) \geqq 0.01$

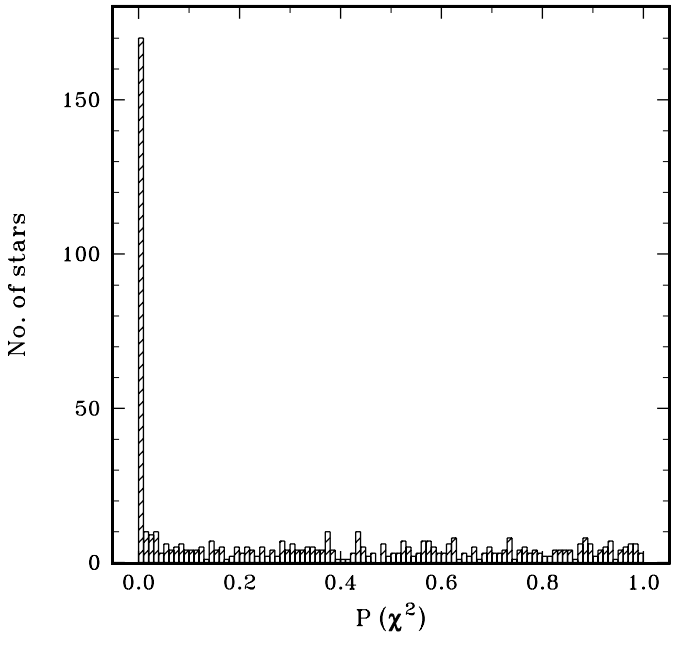

Fig. 4. Distribution of observed $P(\chi^2)$ values for all stars in Tables 1 and 2 with more than one observation (bin size 0.01)

suggest that we have missed about half of the total number of spectroscopic binaries in our own sample. This is to be expected because the detection limit for velocity variability is significantly higher for our fast-rotating F stars, and the time span and number of observations per star are rather lower than in the study by Duquennoy & Mayor.

The 24 double-lined systems consisting of a rapidly-rotating late A star and a sharp-lined cooler secondary are of special interest. As their combined *uvby* indices mimic those of the youngest, early F-type dwarfs, these stars would have appeared in that age group if their binary nature had gone unnoticed. Their derived metallicity would also have been affected by their composite nature, biasing the resulting age-metallicity diagram (AMD).

It has recently been proposed (Wielen et al. 1996) that the scatter in the AMD is the result of diffusion of disk star orbits. According to their model, the true birthplace of a star can be derived from its position in the AMD under the assumption of a single-valued local age-metallicity relation (AMR) and a radial abundance gradient in the disk: The farther a star is off the mean relation, the farther from the solar circle was it supposedly born. As a specific example, since the [Fe/H] of the Sun is 0.17 dex higher than the average for nearby F dwarfs of the same age, it would supposedly have been formed at a galactocentric distance of 6.6 kpc. According to this theory, its orbit would then have been modified by interactions with massive objects in the disk (perhaps giant molecular clouds or massive black holes) so that it reached its present mean distance at $R_0 = 8.5$ kpc after 4.6 Gyr, and with its orbital eccentricity modified again to near its presumably small initial value.

When using F stars to test such an hypothesis (see Nordström et al. 1997), early F stars with high or low abundances are particularly important since they have had the least time to diffuse into the solar neighbourhood from their putative distant birthplaces. Even a few spurious points in the AMD due to unrecognised binaries of the type discussed above could lead to erroneous conclusions. The data presented here will help to avoid such mistakes.

Acknowledgements. The grid of synthetic template spectra computed by Jon Morse, with the model atmosphere programmes and spectral line lists by Robert Kurucz, were key elements in the work presented here, as were the XCSAO package and TODCOR implementations by our CfA colleagues. Financial support to BN and JA from the Carlsberg Foundation, the Danish Natural Science Research Council, and the Smithsonian Institution is gratefully acknowledged.

References

Bastian U., Röser S., 1991-93, PPM Star Catalogues, Vols. I-IV, Astron. Rechen-Institut Heidelberg, Germany

Carlsberg Meridian Catalogue La Palma 1991-94, Observations of positions of stars and planets, Vols. 5-8. Copenhagen University Observatory, Royal Greenwich Observatory and Real Instituto y Observatorio de la Armada en San Fernando

Collins G.W. II, Truax R.J., 1995, ApJ 439, 860

Duquennoy A., Mayor M., 1991, A&A 248, 485

Edvardsson B., Andersen J., Gustafsson B., Lambert D.L., Nissen P.E., Tomkin J., 1993, A&A 275, 101 (E93)

Kurtz M.J., Mink D.J., Wyatt W.F., 1992, in: Worrall DM., Biemesderfer C., Barnes J. (eds.) Astronomical Data Analysis Software and Systems 1, ASPC 25, 432

Latham D.W., 1985, in: Philip A.G.D., Latham D.W. (eds.) Stellar Radial Velocities. L. Davis Press, Schenectady, N.Y., p. 21

Latham D.W., 1992, in: McAlister H., Hartkopf W. (eds.) Complementary Approaches to Binary and Multiple Star Research, IAU Colloq. 135, ASPC 32, 110

Latham D.W., Nordström B., Andersen J., et al., 1996, A&A 314, 864

Magain P., 1987, A&A 187, 323

Mayor M., 1985, in: Philip A.G.D., Latham D.W. (eds.) Stellar Radial Velocities. L. Davis Press, Schenectady, N.Y., p. 35

Nordström B., Andersen J., Olsen E.H., et al., 1997, A&A (submitted)

Nordström B., Latham D.W., Morse J., et al., 1994, A&A 287, 338 (Paper I)

Nordström B., Olsen E.H., Andersen J., et al., 1996, in Burkert A., Hartmann D., Majewski S. (eds.) The History of the Milky Way and its Satellite System, ASPC 112, 145

Olsen E.H., 1983, A&AS 54, 55

Olsen E.H., 1993, A&AS 102, 89

Olsen E.H., 1994a, A&AS 104, 429

Olsen E.H., 1994b, A&AS 106, 257

Strömgren B., 1987, in: Gilmore G., Carswell R.F. (eds.) The Milky Way Galaxy. Reidel, Dordrecht, p. 299

Wielen, R., Fuchs, D., Dettbarn, C., 1996, A&A 314, 438

Wilson O.C., 1941, ApJ 93, 29

Zucker S., Mazeh T., 1994, ApJ 420, 806